# Impact of geoengineering schemes on the global hydrological cycle

**G. Bala*, P. B. Duffy, and K. E. Taylor**

Atmosphere, Earth, and Energy Division, Lawrence Livermore National Laboratory, Livermore, CA 94550

Edited by Robert E. Dickinson, Georgia Institute of Technology, Atlanta, GA, and approved March 12, 2008 (received for review December 12, 2007)

**The rapidly rising $CO_2$ level in the atmosphere has led to proposals of climate stabilization by "geoengineering" schemes that would mitigate climate change by intentionally reducing solar radiation incident on Earth's surface. In this article we address the impact of these climate stabilization schemes on the global hydrological cycle. By using equilibrium climate simulations, we show that insolation reductions sufficient to offset global-scale temperature increases lead to a decrease in global mean precipitation. This occurs because solar forcing is more effective in driving changes in global mean evaporation than is $CO_2$ forcing of a similar magnitude. In the model used here, the hydrological sensitivity, defined as the percentage change in global mean precipitation per degree warming, is 2.4% $K^{-1}$ for solar forcing, but only 1.5% $K^{-1}$ for $CO_2$ forcing. Although other models and the climate system itself may differ quantitatively from this result, the conclusion can be understood based on simple considerations of the surface energy budget and thus is likely to be robust. For the same surface temperature change, insolation changes result in relatively larger changes in net radiative fluxes at the surface; these are compensated by larger changes in the sum of latent and sensible heat fluxes. Hence, the hydrological cycle is more sensitive to temperature adjustment by changes in insolation than by changes in greenhouse gases. This implies that an alteration in solar forcing might offset temperature changes or hydrological changes from greenhouse warming, but could not cancel both at once.**

climate change | global hydrology | radiative forcing | mitigation

The rapid rise in the rate of fossil fuel emission in recent years has revived the discussion of mitigating climate change by "geoengineering" schemes (1–4). The proposed schemes fall into two categories. The first involves reducing the solar radiation absorbed by the climate system by an amount that balances the reduction in outgoing terrestrial radiation because of the increase in the atmospheric $CO_2$ and other greenhouse gases (1, 5–12). The other class of schemes typically removes the atmospheric $CO_2$ and sequesters it in terrestrial vegetation, in deep geologic formations, or in the oceans.

Climate modeling studies have investigated the viability of the first category of schemes. The first equilibrium simulation studies on this subject (13, 14) show that if the model configuration is designed such that the incoming solar radiation ("insolation") is reduced by an appropriate percentage, it could largely mitigate even regional and seasonal climate change from a doubling or quadrupling of $CO_2$, even though the spatial and temporal pattern of radiative forcing from greenhouse gases differs markedly from that of sunlight. These modeling studies find that residual temperature changes in a climate with increased greenhouse gases and appropriately reduced insolation are much smaller than the changes caused by $CO_2$ increases alone.

Further modeling work investigating the impact of climate stabilization schemes on the terrestrial biosphere (15) indicates that climate stabilization would tend to limit changes in vegetation distribution brought on by climate change, but would not prevent $CO_2$-induced changes in Net Primary Productivity (NPP) or biomass. Concerns have also been raised that $CO_2$ effects on ocean chemistry could have deleterious consequences for marine biota because of ocean acidification that is not mitigated by the geoengineering schemes (16).

Investigations of transient climate response to geoengineering by using an intermediate-complexity global climate model that includes an interactive carbon cycle (17) suggest that the climate system responds quickly to artificially reduced solar radiation; hence, there may be little cost to delaying the deployment of geoengineering strategies until such time as "dangerous" climate change is imminent. These studies also find that a failure of the geoengineering scheme could lead to rapid climate change, with warming rates up to 20 times greater than present-day rates.

A limitation of the previous modeling studies is that they do not evaluate the impact of these geoengineering schemes on the global hydrological cycle. A recent observational study (18) shows that there was a substantial decrease in precipitation over land and a record decrease in runoff and discharge into the ocean after the eruption of Mount Pinatubo in 1991. It cautions that a weakened hydrological cycle, including droughts, could arise from geoengineering solutions.

Modeling studies indicate a decline in precipitation in the geoengineered climate (13, 15, 17), relative to an unperturbed control climate. Until now, this decline in precipitation has gone largely unnoticed and has not been investigated in detail. Thus, there has been little recognition of why there should be a reduction in global mean precipitation in the geoengineered climate while there is mitigation in terms of surface temperature change. Larger changes in precipitation for volcanic forcing have been also evident, but not discussed, in earlier modeling studies when the simulated surface temperature changes are the same for $CO_2$ and volcanic forcing (19). There has also been discussion of how the availability of energy, not moisture, controls the overall intensity of the hydrological cycle (20–22)

Our article investigates the sensitivity of the global mean precipitation to $CO_2$ and solar forcings separately and explains the causes for the weakening of the global hydrological cycle in a geoengineered world in which global temperature change has been prevented. We analyze existing equilibrium simulations (15). We emphasize that equilibrium simulations can, in general, only qualitatively predict the transient responses of the climate system. Quantitative results from the model used here will differ from results of other models and from the real climate system. Nonetheless, we believe that the basic phenomenon described here—a greater hydrological sensitivity to solar versus greenhouse forcing—is fundamental and can be understood through a straightforward analysis of the global energy budget.

Author contributions: G.B. designed research; G.B., P.B.D., and K.E.T. performed research; G.B. contributed new reagents/analytic tools; G.B. analyzed data; and G.B., P.B.D., and K.E.T. wrote the paper.

The authors declare no conflict of interest.

This article is a PNAS Direct Submission.

*To whom correspondence should be addressed. E-mail: bala1@llnl.gov.

This article contains supporting information online at www.pnas.org/cgi/content/full/0711648105/DCSupplemental.

**Table 1. Differences in global- and annual-means of key climate variables in the 2×$CO_2$, solar, and stabilized cases, relative to control**

| Experiment | Surface temperature, K | Water vapor, % | Precipitation, % | Net LW flux TOA, W·m$^{-2}$* | Net SW flux TOA, W·m$^{-2}$† | Net flux TOA, W·m$^{2}$‡ |
|---|---|---|---|---|---|---|
| 2×$CO_2$ | 2.42 | 15.2 | 3.7 | −0.54 | 0.46 | −0.08 |
| Solar | −2.40 | −15.2 | −5.8 | 4.86 | −4.79 | 0.07 |
| Stabilized | 0.14 | −2.0 | −1.7 | 3.62 | −3.63 | −0.01 |
| 2×$CO_2$ + solar§ | 0.02 | 0.0 | −2.1 | 4.32 | −4.33 | −0.01 |

*Net longwave (LW) (downward is positive) at the top of the atmosphere (TOA).
†Net shortwave (SW) (downward minus upward) at the TOA.
‡Net flux at the TOA is the sum of net LW and net SW fluxes.
§The last row is the sum of the 2×$CO_2$ and solar cases.

**Model.** The simulations presented here use an atmospheric general circulation model, version 3 of the Community Climate Model (CCM3) developed at the National Center for Atmospheric Research (23), coupled to a terrestrial biosphere model, the Integrated Biosphere Simulator or IBIS (24, 25). The horizontal resolution is ≈2.8° in latitude and 2.8° in longitude. The atmosphere model has 18 levels in the vertical. In this study CCM3 is coupled to a slab ocean-thermodynamic sea ice model, which allows for simplified representation of the interactions with the ocean and sea ice components of the climate system. To ensure realistic sea surface temperatures and ice distributions for the present climate, the slab ocean model employs a spatially and temporally varying prescribed ocean heat transport and spatially varying mixed-layer depth.

**Experiments.** To assess the impacts of increased atmospheric $CO_2$ content on global hydrology, we performed four model simulations (15): (*i*) "Control," with a $CO_2$ content of 355 ppm and incoming solar flux of 1,367 W·m$^{-2}$; (*ii*) "2×$CO_2$," with doubled atmospheric $CO_2$ content (710 ppm), and the same incoming solar flux as the Control simulation; (*iii*) "Solar," with a $CO_2$ content that is the same as Control, but solar flux reduced by 1.8%; and (*iv*) "Stabilized," with doubled atmospheric $CO_2$ content and the solar flux reduced by 1.8%. This reduction in solar luminosity was chosen to approximately offset the surface temperature impacts from a $CO_2$ doubling in this model. Geoengineering schemes would effect this reduction in solar radiation through, for example, the placement of reflecting or scattering devices between the Earth and Sun (2, 8, 10–12), although the uniform fractional reduction in solar insolation imposed in our study would be hard to achieve except in the case of reflectors at L1 point between the Earth and Sun (1, 12). For all experiments, the model was initialized with a state corresponding to present-day conditions. From this initial state, the model was run for at least ≈75 simulated years to approach quasi-equilibrium. The climate statistics presented below are the averaged values over the last 25 years of model simulations. During this period, the global average net flux of energy at the top of the atmosphere is, in absolute terms, <0.1 W·m$^{-2}$, indicating that the system is very nearly in equilibrium (Table 1). In all of the experiments, the drifts in global mean surface temperature during the 25-year period analyzed are of order $10^{-4}$ K, and the interannual variability as measured by the standard deviation of the global mean surface temperature is ≈0.06 K (which is approximately half the variability found when CCM3 is coupled to a full-ocean model). The drift and interannual variability are both very small compared with the differences among simulations analyzed here.

## Results

Compared with the control case, the global- and annual-mean near-surface temperature increases by 2.42 K in the 2×$CO_2$ experiment and decreases by nearly an identical amount in the solar experiment (Table 1). By design, the surface temperature of the stabilized case is very similar to the control case (13–15).

Surface temperature changes in the 2×$CO_2$ and solar cases are significant at the 1% level over all regions of the globe (Fig. 1). The changes are larger over land and high-latitude regions, in agreement with the published literature (26). In the stabilized case the residual temperature changes, although statistically significant over ocean and northern land areas, are much smaller than in the 2×$CO_2$ or solar cases. The vertical distribution of global mean temperature shows a decrease (increase) in lapse rate in the troposphere in the 2×$CO_2$ (solar) case (Fig. 2). We find that the lapse rate changes are dominated by changes in the tropics. The mean stratospheric cooling exceeds 6 K in the 2×$CO_2$ case, and it is <1 K in the solar case. As noted in previous studies (13, 14), the stratospheric cooling is not mitigated in the stabilized case (Fig. 2)

The total water vapor content of the atmosphere is enhanced by 15.2% in the 2×$CO_2$ experiment and reduced by the same amount in the solar case (Table 1). The changes in water vapor content reflect the response of specific humidity to temperature change when the *relative* humidity does not change under climate change (22, 27). The specific humidity response reflects an increase of total water vapor content consistent with the Clausius–Clapeyron relationship: ≈6.5% K$^{-1}$. In the stabilized case there is clear mitigation of climate change in terms of surface temperature and water vapor content of the atmosphere.

In the case of global mean precipitation, however, the mitigation is less exact: precipitation increases by 3.7% for the 2×$CO_2$ case but decreases by 5.8% in the solar experiment (Table 1). Precipitation in the stabilized case is 1.7% less than in the control. This decline is generally pervasive but there are increases in some tropical regions because of a shift in the Intertropical Convergence Zone [supporting information (SI) Fig. S1 and Table S1]. The percentage changes in precipitation do not scale with the Clausius–Clapeyron relationship, and are much smaller than water vapor changes (20–22, 28). This is because, whereas water vapor changes are controlled by the temperature change, precipitation changes, which for changes in $CO_2$ are predicted to be only ≈2% K$^{-1}$ (21), are dictated by changes in the net radiative flux at the surface. The residual change in precipitation that we find in the stabilized case is an indication that the hydrological sensitivity of the climate system depends on the forcing mechanisms.

A metric useful for quantifying hydrological response is the percentage change in precipitation per degree of temperature change (20–22, 29). We refer to this quantity as hydrological sensitivity. The hydrological sensitivities in the model used here are 1.53% K$^{-1}$ for the 2×$CO_2$ case and 2.42% K$^{-1}$ for the solar case. The larger hydrological sensitivity to solar forcing leads to a net decline in global precipitation in the stabilized case relative to the control. In equilibrium, evaporation must equal precipitation, so in the stabilized case there are also decreases in evaporation and the associated latent heat flux (Fig. 3).

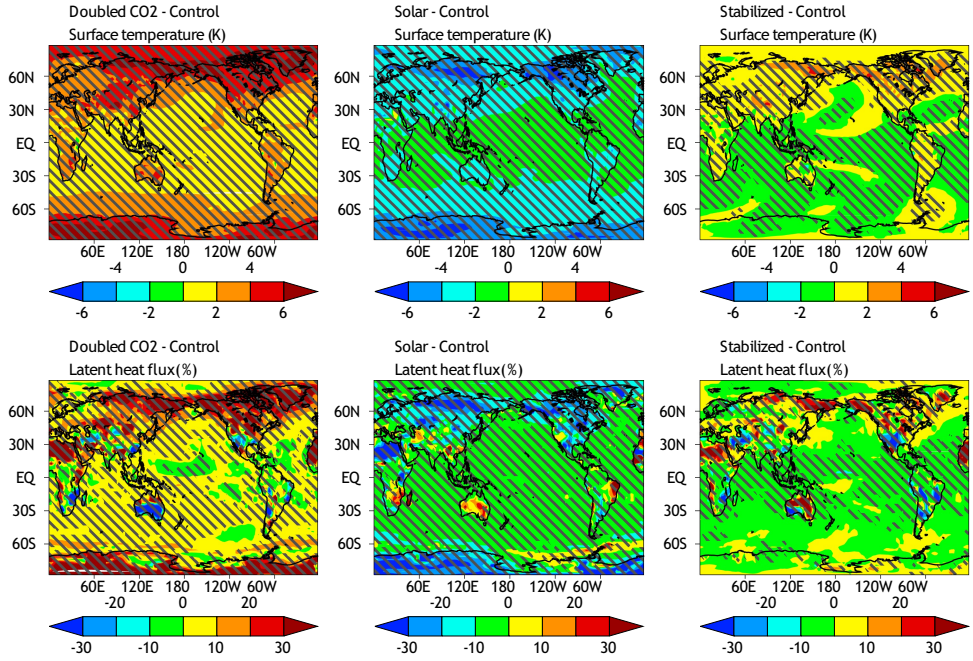


**Fig. 1.** Changes in annual-mean surface temperature (*Top*) and surface latent heat fluxes (*Bottom*) in the $2\times CO_2$, solar, and stabilized cases relative to the control. Hatching indicates the regions where the changes are significant at the 1% level. Significance level was estimating by using a Student *t* test. Temperature changes are large and significant everywhere in the $2\times CO_2$ and solar cases. Although significant over large regions, temperature changes are small in the stabilized case. Surface latent heat flux changes are significant over >61% and 83% the globe in the $2\times CO_2$ and solar cases. There is a general decrease in latent heat flux over most of the regions in the stabilized case relative to the control, suggesting that geoengineering will lead to a weakened hydrological cycle.

To make sense of the global mean changes in precipitation, our approach will be to consider how changes in surface latent heat flux are constrained by the surface energy budget in the global mean. First, however, it is helpful to examine briefly the changes in the annual mean and the seasonal variations of the pattern of latent heat flux (Figs. 1 and 2*b* and Fig. S2). In the $2\times CO_2$ case the latent heat flux generally increases, with larger enhancements in the Northern Hemisphere high-latitude land regions (Figs. 1 and 2*b*). The latent heat flux decreases in the solar case with the magnitude of the reductions being larger than the increases in the $2\times CO_2$ case in the tropics and Southern Hemisphere (Figs. 1 and 2*b*). We find that the percentage changes in evaporation over land are highly variable with >30% changes in the high latitudes and <10% changes in the low latitudes in the $2\times CO_2$ and solar cases. The changes are rather uniform over oceans at <10%. The evaporation changes shown in Fig. 1 are significant at the 1% level for >61% and 83% of the globe in the $2\times CO_2$ and solar experiments, respectively. In the stabilized case, a general decline in latent heat fluxes is evident with statistically significant reductions found mostly in the tropics. Some local increases are seen in high-latitude land regions. Overall, the changes in this case are significant at the 1% level for >42% of the globe, mostly in the tropical region. Changes in the stabilized case show little seasonal variation (Fig. S2), a result that is in agreement with earlier studies (13).

The changes described above are clearly not uniform spatially, and this is also true of the pattern of precipitation changes, which in many areas bear little resemblance to the evaporation changes (Fig. 1 and Fig. S1). Land–ocean contrasts are evident in the responses of both precipitation and evaporation (Table S1), with the fractional responses over land being larger, especially in the $2\times CO_2$ case. At smaller than global scale, it is difficult to see similarities in the rather noisy patterns of change in precipitation and latent heat flux.

Why are the hydrological sensitivities different for greenhouse versus solar forcing? Differences in the vertical distribution of radiative forcing for $2\times CO_2$ and solar cases (30) lead to a simple explanation. Radiative forcing by $CO_2$ mainly heats the troposphere (in a direct sense), whereas solar forcing mainly heats the surface (30). Therefore, the energy available for latent and sensible heat fluxes (at the surface) is more strongly affected by solar forcing than by greenhouse forcing that has the same magnitude at the tropopause. This leads directly to the reduced evaporation and precipitation in the stabilized case.

A rigorous explanation requires quantitative consideration of vertical fluxes of energy at the surface. The time-mean, globally averaged surfaced energy flux differences between any two equilibrium states must sum to zero:

$$\Delta R + \Delta S - \Delta L - \Delta H = 0, \qquad [1]$$

where $\Delta R$, $\Delta S$, $\Delta L$, and $\Delta H$ represent the differences in longwave radiation, shortwave radiation, latent heat, and sensible heat, respectively. Here, we use this formulation to assess changes in the $2\times CO_2$, solar, and stabilized cases relative to the control case. The sign convention is that downward fluxes are positive for radiation and negative for latent and sensible heat. It is useful to resolve the radiative fluxes into "forcing" and "response" components, where the forcing is usually defined to be the instantaneous impact of some perturbation on radiation [but more generally accounts for any relatively fast radiative responses unrelated to changes in global temperature (31)]. Then Eq. **1** becomes

$$F + \Delta R_r + \Delta S_r - \Delta L - \Delta H = 0, \qquad [2]$$

where $F$ is the sum of shortwave and longwave radiative forcing and the subscripts $r$ indicate that the terms represent only the response component of the change in radiation.

In our model the surface forcing is approximately $-3$ W·m$^{-2}$ in the solar case, but only a few tenths of a W·m$^{-2}$ in the $2\times CO_2$ case. Because, to a good approximation, the radiative responses are independent of the forcing mechanism (30), $\Delta R_r$ has the same

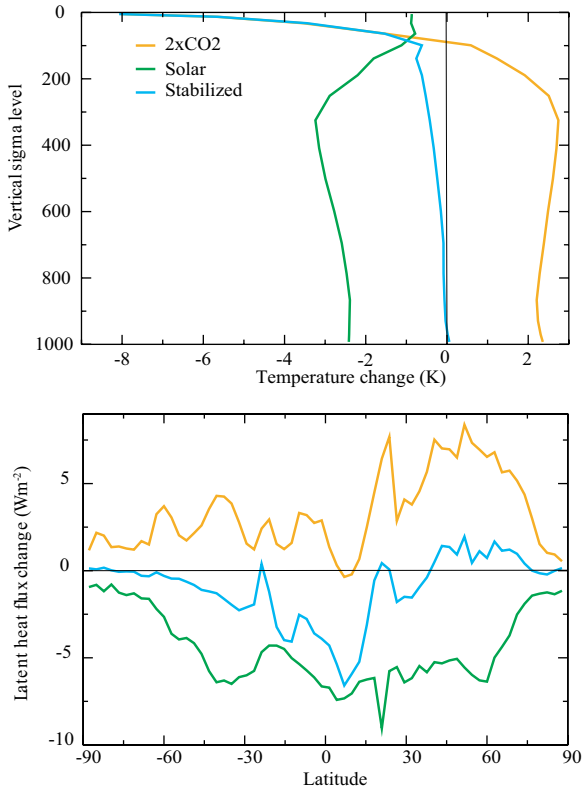


**Fig. 2.** Changes in the vertical profile of the global- and annual-mean temperature (*Upper*), and in the meridional distribution of zonal mean latent heat fluxes (*Lower*) in the $2\times CO_2$, solar, and stabilized experiments relative to the control. The lapse rate in the $2\times CO_2$ (solar) case increases (decreases). The large stratospheric cooling in the $2\times CO_2$ case is not mitigated by a reduction in solar insolation. As evidenced by reduced evaporation, particularly in the tropics, the hydrological cycle is weakened in the stabilized case relative to the control.

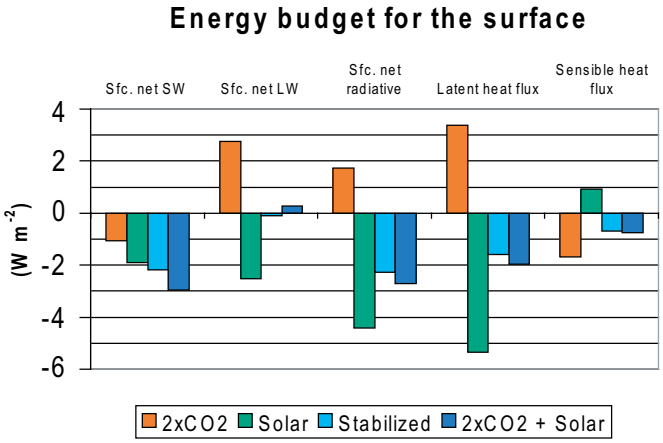


**Fig. 3.** Differences in surface energy fluxes, averaged globally and annually, in the $2\times CO_2$, solar, and stabilized cases, relative to control. ''Sfc. net SW'' refers to the net surface absorption (incident minus reflected) of solar radiation, and ''Sfc. net LW'' refers to net absorption (downward minus upward) of longwave radiation at the surface. ''Sfc. net radiative'' represents the change in the absorbed total radiative flux at the surface. The changes in surface latent and sensible heat fluxes are positive upward.

magnitude in both cases (solar and $2\times CO_2$), but has opposite signs. This is true also of the shortwave response, $\Delta S_r$. Because in these experiments the separate responses to different forcings are approximately additive, the radiative response terms in Eq. **2** can be neglected for the stabilized case, and the net radiative flux at the surface ($\approx -2.5$ W·m$^{-2}$; Fig. 3) is just the sum of the individual radiative forcings. This means that in the stabilized case the radiative response is negligible, and surface radiative forcing must be balanced by changes in latent and sensible heat:

$$\Delta L + \Delta H \approx F. \qquad [3]$$

It should not be surprising that the surface radiative *response* is approximately zero in the stabilized case, because the variables affecting radiative transfer (temperature, water vapor, and clouds) do not change much relative to the control case (see Fig. 2 for the vertical temperature structure). Applying Eq. **3**, we find that the negative surface radiative forcing, caused primarily by the solar forcing, must be largely balanced by a decrease in the sum of latent and sensible heat fluxes.

A similar analysis of the atmospheric energy budget leads to a complementary result: if the equilibrium global mean temperature remains unchanged, changes in the heating rate of the atmosphere because of radiative forcing must be balanced by changes in sensible plus latent heat release. The radiative forcing of the atmosphere is the difference between the radiative forcing at the top of the atmosphere and the surface. In the stabilized case, this is equal and opposite to the radiative forcing at the surface because the radiative forcing at the top of the atmosphere is zero. A decrease in the sum of sensible and latent heat fluxes from the surface to the atmosphere balances this atmospheric radiative forcing.

Eq. **3** does not constrain the *partitioning* between the latent and sensible heat fluxes that together must balance the radiative forcing. In the control climate the ratio of the sensible to latent heat flux (i.e., the Bowen ratio) is $\approx 0.2$, so it seems likely that under perturbed conditions the latent heat flux response will dominate (as it does in the model used here). This is true not only of the stabilized case, but also in the individual forcing runs ($2\times CO_2$ and solar) where, in fact, the sensible and latent heat flux changes are of opposite sign (Fig. 3). The dominance of latent heat flux changes relative to sensible heat flux changes in Eq. **3** means that, in general, when a combination of offsetting radiative forcings leads to an equilibrium climate in which the global mean surface temperature is unchanged, changes in precipitation can be predicted from knowledge of the surface or atmospheric radiative forcing alone. In fixed sea surface temperature (SST) experiments, however, only the radiative forcing of the atmosphere is a good predictor of precipitation changes. In this case, the radiative forcing of the atmosphere must be balanced mostly by changes in latent heating, whereas the radiative forcing of the surface may not imply any change in evaporative cooling because it can be balanced by changes in ocean heat storage.

## Discussion

In our experiments, climate (i.e., temperature) sensitivity is roughly the same for the two different forcing mechanisms, but hydrological sensitivity is different. In the model used here, the temperature response to a reduction in insolation is of nearly equal magnitude to the response to an increase in $CO_2$ having the same nominal radiative forcing. However, the hydrological sensitivity to increasing atmospheric $CO_2$ is 1.5% K$^{-1}$, whereas for a reduction in solar radiation, it is 2.4% K$^{-1}$. Thus, shortwave forcing, which primarily impacts (in an immediate sense) the surface, is more effective in driving changes in global evaporation/precipitation than is a similar magnitude of forcing by $CO_2$, which mostly impacts the atmosphere. The reason for this, in essence, is that if climate is warmed by an increase in insolation, the surface sees an increase in incident shortwave plus an

increase in downwelling longwave from the warmer atmosphere above. By contrast, if the climate is warmed by increasing greenhouse gases, the surface sees only the increased longwave flux (to a first approximation). The differences in surface radiation in these two cases lead to different responses in evaporation and, consequently, also in precipitation.

The conclusions reached here rest on the approximate validity of Eq. **3**, in which radiative responses at the surface are neglected when surface temperature does not change. At the top of the atmosphere (TOA), it is known from modeling studies (30–33) that the radiative response is approximately linearly related to the global mean surface temperature change. This is, in fact, why, when the radiative forcing is carefully defined (31), a model's equilibrium climate sensitivity (i.e., the ratio of global mean temperature change to the global mean forcing) is approximately independent of the characteristics of the forcing (e.g., spatial or temporal pattern). Because the vertical profiles of temperature, humidity, and clouds determine both the surface and TOA radiative fluxes, it would be surprising if one were to change but the other did not. The generally accepted empirical result that the TOA radiative response is a function of the global mean surface temperature implies, therefore, that the surface radiative response will be small if the surface temperature does not change. Thus, Eq. **3** should hold across models, as should our conclusions.

Our results are also consistent with earlier modeling experiments that showed a decrease in precipitation for an increase in atmospheric $CO_2$ when SSTs were fixed (34, 35). This response is similar to our stabilized case in that greenhouse gases increase without an associated change in the surface temperature. In these experiments, as in our experiment, the enhanced heating of the atmosphere because of the $CO_2$ forcing is balanced by a reduction in latent heat release (reduced precipitation), since the radiative response of the system must be small because of the fixed SST constraint. At the surface, in these experiments, the ocean serves as an infinite heat sink, taking up sufficient heat to balance reduced cooling by evaporation.

Because the model used here lacks a dynamic ocean and sea ice model, the transient effects of climate change and its impact on global hydrology are not assessed in this study. It is possible, however, to apply our analysis to a hypothetical transient simulation in which temperature changes that would result from gradual increases in greenhouse gases were successfully mitigated (in terms of global mean temperature) by gradual increases in sulfate aerosol concentrations, for example. Under these conditions the climate might not remain in true equilibrium because some regions might warm whereas others might cool (although the global mean would not change). There could also be exchanges of heat with the oceans. To the extent Eq. **3** holds, as applied to the atmosphere, we would expect to find a gradual decrease in the global mean precipitation rate, consistent with our equilibrium theory.

The differing hydrological sensitivities for greenhouse versus solar forcings have clear implications for the proposed geoengineering schemes that attempt to reduce the incoming solar radiation by injecting sulfate aerosols into the stratosphere or by placing mirrors or reflectors in space. Although these schemes could possibly mitigate, to a degree, the harmful effects of rising surface temperature, they will lead to a reduction in global mean precipitation and evaporation.

Our investigation has focused only on the *global* hydrology; we have not analyzed regional details of hydrological changes caused by geoengineering because, in all cases, the changes in precipitation are quite small relative to interannual variability at the regional scale (Fig. S1). We find, for example, that for a doubling of $CO_2$, the precipitation changes are significant at the 1% level over only 46% of the globe. For the stabilized case, this fraction drops to 33%. Precipitation minus evaporation ($P - E$) is an approximate measure of water availability and droughts. Statistical significance of changes in this quantity is achieved over only 25% of the globe in the stabilized case (Fig. S1). Longer integrations and high-resolution modeling will be required to provide confidence in regional scale changes in runoff, soil moisture, streamflow, and water resources. We also have not investigated daily and hourly rates (i.e., intensity) of precipitation, although there is evidence that climate change will affect the frequency and intensity of storms, with changes in precipitation intensity within individual storms expected to scale with changes in atmospheric water vapor content (20, 29).

Besides a reduction in the rate of global mean water cycling in the geoengineered world, as pointed out in our study, there are many reasons not to engage in geoengineering schemes for climate stabilization. Geoengineering of this kind will not mitigate the harmful effects of ocean acidification because the geoengineered world would still have higher concentration of atmospheric $CO_2$. Some stabilization schemes could adversely impact the ozone layer. $CO_2$-induced climate change would last multiple centuries because the atmospheric residence time scale of $CO_2$ is a few centuries. Consequently, if geoengineering schemes are implemented, the commitments would have to be maintained over many centuries (16). It would be difficult to develop an international consensus to engage in a long-term large-scale geoengineering project (36), and technical failure of a stabilization scheme could be catastrophic (17).

**ACKNOWLEDGMENTS.** We thank Drs. D. Lobell, B. Santer, and P. Caldwell for their interest in this work and for reviewing the original manuscript. This work was supported by the U.S. Department of Energy, Lawrence Livermore National Laboratory, Contract DE-AC52–07NA27344.

1. Angel R (2006) Feasibility of cooling the Earth with a cloud of small spacecraft near the inner Lagrange point (L1). *Proc Natl Acad Sci USA* 103:17184–17189.
2. Crutzen PJ (2006) Albedo enhancement by stratospheric sulfur injections: A contribution to resolve a policy dilemma? *Climatic Change* 77:211–219.
3. Gail WB (2007) Climate control. *IEEE Spectrum* 44:20–25.
4. Wigley TML (2006) A combined mitigation/geoengineering approach to climate stabilization. *Science* 314:452–454.
5. President's Scientific Advisory Committee (PSAC) (1965) *Restoring the Quality of Our Environment. Appendix Y4, Atmospheric Carbon Dioxide* (The White House, Washington DC), Report by the U.S. President's Scientific Advisory Committee, pp 111–133.
6. Budyko MI (1977) *Climatic Changes* (American Geophysical Union, Washington, DC).
7. Seifritz W (1989) Mirrors to halt global warming. *Nature* 340:603–603.
8. NAS (1992) *Policy Implications of Greenhouse Warming: Mitigation, Adaptation and the Science Base* (National Academy Press, Washington DC), pp 433–464.
9. Watson RT, Zinyowera MC, Moses RH, Dokken DJ (1995) *Climate Change 1995.* Intergovernmental Panel on Climate Change, United Nations Environ Program/World Meteorological Organization (Cambridge Univ Press, New York), pp 799–822.
10. Flannary BP, Kheshgi H, Marland G, MacCraken MC (1997) *Engineering Response to Global Climate Change* (Lewis Publishers, University City, MO), pp 403–421.
11. Teller E, Wood L, Hyde R (1997) *UCRL-231636/UCRL JC 128715* (Lawrence Livermore National Laboratory, Livermore, CA).
12. Early JT (1989) The space based solar shield to offset greenhouse effect. *J Brit Interplanet Soc* 42:567–569.
13. Govindasamy B, Caldeira K (2000) Geoengineering Earth's radiation balance to mitigate CO2-induced climate change. *Geophys Res Lett* 27:2141–2144.
14. Govindasamy B, Caldeira K, Duffy PB (2003) Geoengineering Earth's radiation balance to mitigate climate change from a quadrupling of CO2. *Global Planet Change* 37:157–168.
15. Govindasamy B, *et al.* (2002) Impact of geoengineering schemes on the terrestrial biosphere. *Geophys Res Lett* 29:2061.
16. Bengtsson L (2006) Geo-engineering to confine climate change: Is it at all feasible? *Climatic Change* 77:229–234.
17. Matthews HD, Caldeira K (2007) Transient climate-carbon simulations of planetary geoengineering. *Proc Natl Acad Sci USA* 104:9949–9954.
18. Trenberth KE, Dai A (2007) Effects of Mount Pinatubo volcanic eruption on the hydrological cycle as an analog of geoengineering. *Geophys Res Lett* 34:L15702.
19. Pollack JB, *et al.* (1993) GCM simulations of volcanic aerosol forcing. 1. Climate changes induced by steady-state perturbations. *J Climate* 6:1719–1742.
20. Trenberth KE (1999) Conceptual framework for changes of extremes of the hydrological cycle with climate change. *Climatic Change* 42:327–339.
21. Held IM, Soden BJ (2006) Robust responses of the hydrological cycle to global warming. *J Climate* 19:5686–5699.

22. Allen MR, Ingram WJ (2002) Constraints on future changes in climate and the hydrologic cycle. *Nature* 419:224–232.
23. Kiehl JT, *et al.* (1998) The National Center for Atmospheric Research Community Climate Model: CCM3. *J Climate* 11:1131–1149.
24. Foley JA, *et al.* (1996) An integrated biosphere model of land surface processes, terrestrial carbon balance, and vegetation dynamics. *Global Biogeochem Cycles* 10:603–628.
25. Kucharik CJ, *et al.* (2000) Testing the performance of a dynamic global ecosystem model: Water balance, carbon balance, and vegetation structure. *Global Biogeochem Cycles* 14:795–825.
26. Meehl GA, *et al.* (2007) *Climate Change 2007: The Physical Science Basis. Contribution of Working Group I to the Fourth Assessment Report of the Intergovernmental Panel on Climate Change*, eds Solomon S, *et al.* (Cambridge Univ Press, Cambridge, UK).
27. Ross RJ, Elliott WP, Seidel DJ, Participating AMIP-II Modeling Group (2002) Lower-tropospheric humidity-temperature relationships in radiosonde observations and atmospheric general circulation models. *J Hydrometeorol* 3:26–38.
28. Boer GJ (1993) Climate change and the regulation of the surface moisture and energy budgets. *Climate Dyn* 8:225–239.
29. Trenberth KE, Dai AG, Rasmussen RM, Parsons DB (2003) The changing character of precipitation. *Bull Am Meteorol Soc* 84:1205–1217.
30. Hansen J, Sato M, Ruedy R (1997) Radiative forcing and climate response. *J Geophys Res Atmos* 102:6831–6864.
31. Hansen J, *et al.* (2005) Efficacy of climate forcings. *J Geophys Res Atmos* 110:D18104.
32. Cox SJ, Wang WC, Schwartz SE (1995) Climate response to radiative forcings by sulfate aerosols and greenhouse gases. *Geophys Res Lett* 22:2509–2512.
33. Ramaswamy V, Chen CT (1997) Linear additivity of climate response for combined albedo and greenhouse perturbations. *Geophys Res Lett* 24:567–570.
34. Mitchell JFB (1983) The seasonal response of a general-circulation model to changes in CO2 and sea temperatures. *Q J R Meteorol Soc* 109:113–152.
35. Yang FL, Kumar A, Schlesinger ME, Wang WQ (2003) Intensity of hydrological cycles in warmer climates. *J Climate* 16:2419–2423.
36. Schneider SH (2001) Earth systems engineering and management. *Nature* 409:417–421.